Effect of Proton Irradiation on the Mechanical Property of Nano-Porous Zirconium Oxide Layer Fabricated by Anodization Technique

Jung Woo Kim [a*], Yang Jeong Park [a], Jaewoo Lee [a] and Sung Oh Cho [a]
[a] *Department of Nuclear and Quantum Engineering, KAIST, Daejeon306701, Republic of Korea*
* *wjddn3703@kaist.ac.kr*

1. Introduction

In a nuclear power plant, the nuclear cladding that seals the fuel should have excellent mechanical properties and oxidation resistance. Zirconium alloy, which is in conformity with its characteristics, is considered to be one of the most popular cladding materials with the advantage of small neutron absorption cross section. Since the Fukushima nuclear accident, studies have focused on the development of fuel cladding that can withstand the high temperatures in a loss of coolant accident (LOCA) environment. Heightened safety concerns have led to increased focus on the improvement of the claddings currently in use in the nuclear field.

Recent research has been focused on silicon-carbide (SiC) materials, which exhibit relatively superior oxidation resistance and heat transfer efficiency than Zr Alloy. However, the low impact strength of ceramic materials and an axial swelling[1] in the irradiation environment are still problems to be solved. As another approach to improve the accident tolerant fuel cladding, many studies have developed a coating layer on the surface of Zr alloy with a metal having high oxidation resistance. Weight gain of the Zr alloy coated with TiN and Ti1-xAlxN complex was 6 times smaller than the pristine Zr alloy at 360 °C [2]. In addition, it was confirmed that the thickness of oxidation layer grown at 1200 °C in the steam atmosphere was 25 times lower in the case of Cr-coated Zr alloy tubes[3]. However, the degradation of the material properties due to irradiation damage in the normal operating condition of the reactor is inevitable. The irradiation resistance of the developed coating material also has to be proved, but the described literature have not been evaluated yet. In particular, mechanical degradation due to irradiation damage is a more serious problem to be considered. It is important to evaluate the integrity between the fabricated coating layer and the Zr base. Especially, irradiation-induced axial growth results in a strain mismatch between the coating material and the Zr base material, suggesting the necessity of constructing the integrity of the coating material under the irradiation damage[4].

In this study, the irradiation resistance of the porous oxide layer fabricated on the Zr alloy surface through anodization is evaluated. Irradiation damage is induced by utilizing a proton source and the mechanical properties of the oxide layer are examined. As an approach of measuring the mechanical properties, prepared pillars with microscopic size is compressed.

2. Methods and Results

2.1 Methods

2.1.1 Sample preparation

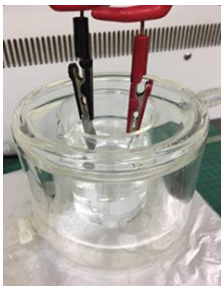

Fig. 1. Anodization system

Ultrasonic cleaning of Zircaloy (Zr-0.1Fe-1.0Nb-1.0Sn wt%) specimens in Acetone (10 min), Ethanol (10 min), and deionized water (20 min) took place after mechanical polishing. Figure 1 shows the anodization system. Anodization was performed using a Zircaloy specimen as the working electrode and a Pt sheet as the counter electrode. The electrolyte used for the anodization experiment was prepared from ethylene glycol based with NH_4F and H_2O solute. The thickness of the nanoporous oxide layer was manipulated by an applied voltage from 30 to 150 V during 3 ~ 15 min.

2.1.2 Proton irradiation

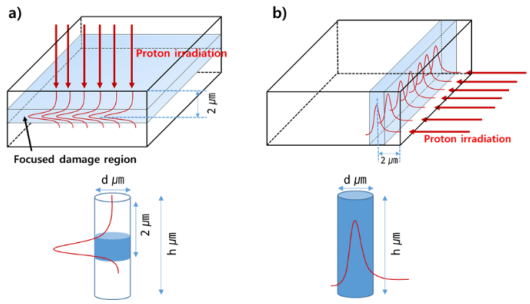

Fig. 2. Schematic of perpendicularly (a), and horizontally (b) irradiated cases

Anodized specimens were perpendicularly and horizontally irradiated with 200 keV proton with $1x10^{18}$ H^+/cm^2 fluence condition at the Advanced Radiation Technology Institute (KAERI). Figure 2 shows schematics of two cases considering perpendicular and horizontal direction.

Proton dpa (displacement per atom) profile was calculated by Stopping and Range of Ions in Matter

(SRIM) code. The displacement energies used for Zr, O and F were 25, 28, 25 eV, respectively [5]. The density of fabricated oxide layer used for the simulation was 3.212 g/cm^3.

2.1.3 Pillar fabrication and compassion test

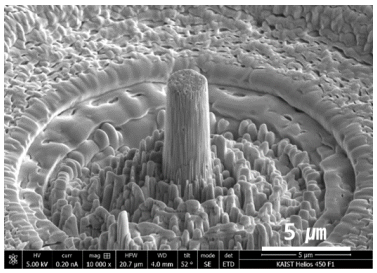

Fig. 3. Micro pillar for compression test

Micro-pillars with diameters of 2 μm and aspect ratio about 3 were fabricated utilizing Focused Ion Beam(Helios 450 F1) using a Ga^+ beam at 30 kV. A final milling current was 0.79 nA (See Figure 3). Each of the unirradiated and irradiated pillars was subjected to a compression test using a Pico-Indenter (PI-87 Hysitron) at a strain rate of 1×10^{-3} s^{-1}.

2.1.4 Characteristics of Microstructure

Microstructures were examined to observe what changes occurred in the microstructure of the oxide layer after induced irradiation damage of proton. TEM (Transmission Electron Microscope) apparatus (Talos F200X) with an accelerating voltage of 200 kV was utilized to observe diffraction patterns and high resolution images that implying the degree of amorphousness and a lattice distance of crystalline structure respectively.

2.2 Results

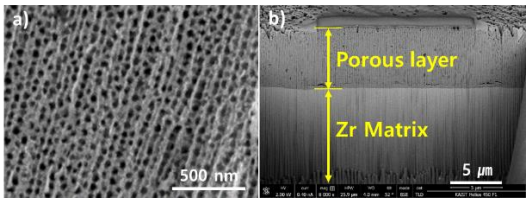

Fig. 4. (a) Top surface SEM and (b) Cross-Sectional BSE images of nano-porous oxide layer fabricated by anodization

The anodization can form an oxide layer having a nano-porous structure on the surface, which can be manufactured by controlling the size and the thickness of the pores. Depending on the type of electrolyte, applied voltage, current, duration time, and temperature, the shape of the surface varies from tubes to sponges [6, 7]. The anodization condition required to fabricate the oxide layer with a uniform and sufficient depth of porous structure should be optimized by taking into account these parameters. Figure 4 shows the surface and cross-sectional images produced by applying anodization. A uniform and well-ordered pore with an average diameter of 50 nm was produced (Fig. 4a). The Zircaloy matrix and the fabricated nanostructured oxide layer are distinguished by contrast (Fig. 4b). It is noteworthy that the fabricated porous layer adheres well to the Zircaloy matrix and has a sufficient and uniform thickness.

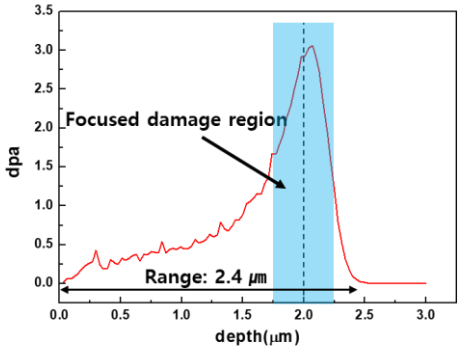

Fig. 5. SRIM code calculation of proton irradiation

From the surface of fabricated oxide layer, the range and displacements per atom(dpa) of the proton irradiation were calculated in Fig. 5. The area with high dpa value was shaded. The dpa profile implies significant irradiation damage occurs in the vicinity of 2 μm.

Micro-pillars for compression testing can be fabricated in a variety of aspect ratios ranging from 1 to 4 [8, 9]. The effect of the aspect ratio on the mechanical behavior is almost negligible and the stress and strain values measured on the actual size of the pillar, rather than on the ratio, are determined[10]. When deriving the mechanical properties, the material of the substrate supporting the pillars should also be considered[11]. In order to measure the mechanical properties of the oxide layer fabricated by anodization, sufficient depth of the oxide layer substrate should be guaranteed when prepared pillars are compressed. In this experiment, the aspect ratio of the compressed pillar was determined to be 3, and the pillar height was set to 6 μm in consideration of the substrate effect in the oxide layer grown to a thickness of 10 μm.

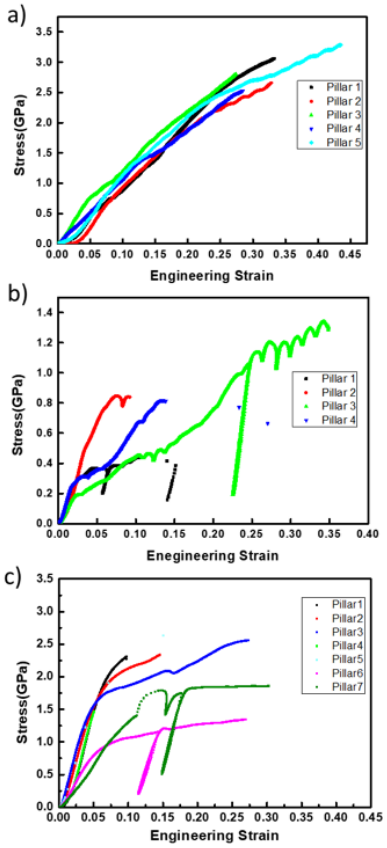

Fig. 6. Compression test results of unirradiated pillar (a), irradiated perpendicularly (b) and horizontally (c)

As a result of the compression test of the unirradiated pillar, the fracture stress and strain were measured at 3 GPa and 0.3 respectively (Fig. 6a). where the stress is retained with increasing strain point exists intermittently apart from the strain/stress slope. This is because the compressed pillar has discontinuous porous structure, not monolithic. This behavior might be caused by the breakage of individual pores before stress is applied to the entire pillar. Fig. 6b shows results of the compression test of the irradiated pillar. There was no reproducibility of mechanical behavior for each pillar. While there is a pillar with strain values similar to the pillar before proton irradiation, such as pillar 3, pillar 1 demonstrates complete mechanical degradation of material. Fracture stress was commonly reduced comparing with the case of unirradiated pillar. The presence of a focused damage region induced by proton irradiation, provided a region that easily concentrates stress when applying compressive stress. If a proton is irradiated horizontally, the effect of irradiation damage can be observed more clearly, since the irradiation damage is evenly received throughout the pillar, resulting in no stress concentration. In the compression test of irradiated pillar, the yield point appears, which is more likely to show mechanical behavior of metal material. That is, the material becomes more ductile. It can be clearly seen that the initial elastic mode changes to plastic deformation at the yield point.

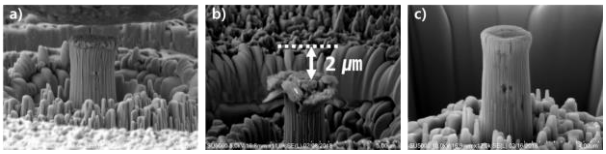

Fig. 7. Fracture morphologies of unirradiated pillar (a), irradiated perpendicularly (b) and horizontally (c)

Figure 7 shows the fracture morphologies after the compression test. The fracture of unirradiated pillar occurs with sequential compression from the top surface. On the other hand, irradiated pillar was observed to be broken around a certain height. The dashed line in Figure 7b is the upper position of the pillar before being compressed. The fracture occurs around this area at 2 μm away from the upper position of the pillar. This location corresponds to the region that induced the most irradiation damage value in the calculation of the SRIM Code. Prior to conducting the compression test, this neighborhood might be more vulnerable than the other areas because of focused high dpa. Therefore, the primary reason that the fracture stress is decreased in general compared to before the proton irradiation is that a weak position exists. When a compressive stress is applied, it can be judged that the stress is concentrated at this position and that breakage has occurred more easily. Unlike the brittle characteristics of well-known ceramic materials, cracks were not commonly observed in the fracture morphologies before and after the proton irradiation (Fig. 7a, c). This means that the pillars were subjected to plastic deformation until fracture failure.

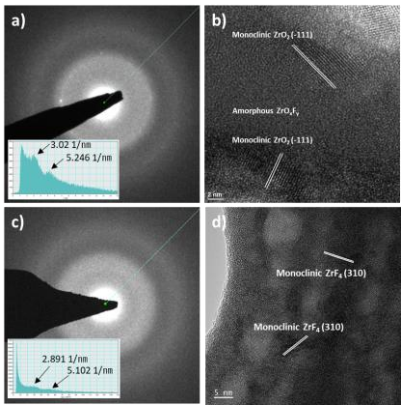

Fig. 8. Diffraction pattern of unirradiated (a), irradiated (c) case and high resolution image of unirradiated (b), irradiated (d) case

The cause of plastic deformation was observed through TEM analysis in the microstructure. Figure 8a and b show diffraction pattern of unirradiated and irradiated cases. It can be seen that both unirradiated and irradiated ceramic layer have an amorphous structure. In the amorphous system, when applied an external stress to the material, it would be easier for the atoms to break bonds and bond to other atoms, which will result in

ductile properties rather than brittle properties. The increase in the distance between the atoms after the proton irradiation is shown in the inset of Figure 8. It can be concluded that the free volume in the material enlarges due to the proton irradiation and the more ductile characteristic appears. Most regions of ceramic layers fabricated by anodization are amorphous structures, but the crystal lattice was observed in the area surrounding the nano pores. In the Figure 8c and d, it was found that monoclinic ZrO_2 replaced to ZrF_4 with the same crystalline structure by the proton irradiation. In general, the irradiation damage can create defects in the crystal structure. Thus, It is thought that the defect is generated in the monoclinic ZrO_2 lattice by proton irradiation and the F element in the amorphous matrix is diffused and combined with the Zr element to form the fluoride phase. The increase in the modulus of elasticity after the proton irradiation in the stress/strain curve was judged to be due to the phase transformation to ZrF_4, which has a relatively high strength.

3. Conclusions

To develop an ATF cladding, many studies have adopted an approach to produce coating materials on the Zircaloy surface. The anodization technique facilitates the fabrication of an oxide layer with a nanostructure on the cladding surface with a simple process. In this study, the mechanical properties were measured in the microscopic scale to observe the effect of proton irradiation on the ceramic layer fabricated on the Zircaloy surface through the anodization. The nano-porous structure with average diameter 50 nm and thickness of 10 μm was uniformly fabricated. The compression test was performed to a pillar made of 2 μm in diameter with an aspect-ratio approximately 3 at the oxidation layer before and after the proton irradiation. Unlike the general characteristics of ceramics, the fabricated layer showed plastic behavior with high fracture stress and more ductile after proton irradiation. The nano-structured oxide layer, which has ductile properties with high strength of ceramic materials, can be expected to be utilized in engineering materials in various fields.

REFERENCES

[1] Mohd Idzat Idris *et al*., “Neutron irradiation swelling of SiC and SiCf/SiC for advanced nuclear applications”, Energy Procedia 71 (2015) 328-336
[2] E. Alat et al., “Multilayer (TiN, TiAlN) ceramic coatings for nuclear fuel cladding”, Journal of Nuclear Materials 478 (2016) 236-244
[3] H.-G. Kim *et al*., “Adhesion property and high-temperature oxidation behavior of Cr-coated Zircaloy-4 cladding tube prepared by 3D laser coating”, Journal of Nuclear Materials 465 (2015) 531-539
[4] Y. Lee *et al*., “Mechanical analysis of surface-coated zircaloy cladding”, Nuclear Engineering and Technology 49 (2017) 1031-1043
[5] R.E. Stoller, G.R. Odette, B.D. Wirth, “Primary damage formation in bcc iron”, J. Nucl. Mater. 251 (1997) 49-60
[6] Ho Seon Ahn *et al.*, “Pool boiling CHF enhancement by micro/nanoscale modification of zircaloy-4 surface”, Nuclear Engineering and Design 240 (2010) 3350–3360
[7] Rejin Raghavan *et al*., “Mechanical behavior of intragranular, nano-porous electrodeposited zinc oxide”, Thin Solid Films 578 (2015) 174–179
[8] Yano, Kayla Haruko. "In Situ TEM Micropillar Compression Testing in Irradiated Oxide Dispersion Strengthened Alloys" 2017, Boise State University Theses and Dissertations, 1320
[9] Kiener *et al*., “In situ nano-compression testing of irradiated copper”, Nat Mater. ; 10(8): 608–613
[10] C.R. Mayer et al., “Anisotropy, size, and aspect ratio effects on micropillar compression of Al-SiC nanolaminate composites”, Acta Materialia 114 (2016) 25-32
[11] Huiyang Fei *et al*., “Evaluation of Micro-Pillar Compression Tests for Accurate Determination of Elastic-Plastic Constitutive Relations”, J. Appl. Mech 79(6), 061011 (Sep 17, 2012) (9 pages)